Available online at www.sciencedirect.com
SCIENCE DIRECT®
International Journal of Pressure Vessels and Piping 82 (2005) 407–416
INTERNATIONAL JOURNAL OF Pressure Vessels and Piping
www.elsevier.com/locate/ijpvp

Plastic collapse of pipe bends under combined internal pressure and in-plane bending

Andrew Robertson, Hongjun Li, Donald Mackenzie*

Department of Mechanical Engineering, University of Strathclyde, James Weir Building, 75 Montrose Street, Glasgow, Scotland G1 1XJ, UK

Received 30 October 2003; revised 20 August 2004; accepted 15 September 2004

Abstract

Plastic collapse of pipe bends with attached straight pipes under combined internal pressure and in-plane closing moment is investigated by elastic–plastic finite element analysis. Three load histories are investigated, proportional loading, sequential pressure–moment loading and sequential moment–pressure loading. Three categories of ductile failure load are defined: limit load, plastic load (with associated criteria of collapse) and instability loads. The results show that theoretical limit analysis is not conservative for all the load combinations considered. The calculated plastic load is dependent on the plastic collapse criteria used. The plastic instability load gives an objective measure of failure and accounts for the effects of large deformations. The proportional and pressure–moment load cases exhibit significant geometric strengthening, whereas the moment–pressure load case exhibits significant geometric weakening.

Keywords: Pipe bend; Plastic collapse criterion; Plastic instability; Geometric non-linearity

1. Introduction

Industrial piping is subject to many different kinds of loading but for the purposes of code design three categories of load type are defined: sustained load, occasional load and expansion load. Sustained loads arise from the mechanical forces acting on the system under design conditions and include pressure, self-weight, fluid weight and insulation weight. Occasional loads also arise from mechanical forces but are expected to occur during only a small proportion of the plant life, such as intermittent operational loads or overload due to fault conditions. Expansion loads arise when the piping system experiences changes in temperature over the operating cycle. This causes cyclic thermal expansion of the piping material, inducing thermal stress in the components and reaction forces at connections to plant, supports and anchors.

Piping design codes seek to prevent failure due to the action of these loads. The codes guard against failure through appropriate choice of material and limiting the loads acting on the system. Three main types of failure are considered in routine design: gross plastic deformation, incremental plastic collapse (ratchetting) and fatigue. Gross plastic deformation is the fundamental ductile failure mode associated with static loading. It is prevented by restricting the magnitude of sustained and occasional loads. Ratchetting is a ductile failure mode associated with cyclic loading. It is prevented by limiting the magnitude of the static sustained loads plus the cyclic thermal expansion loads. Fatigue failure may occur at stress concentrations in the system after a finite number of load cycles, which in turn may determine the design life of the piping system.

The magnitude of thermal stresses resulting from cyclic loading is a function of the flexibility of the system. Ratchetting problems can be minimised by ensuring the system has sufficient flexibility to absorb thermal expansion without inducing excessive stresses, deformations or connection forces in the system. System flexibility is enhanced by incorporating flexible components in the system. These may be specific expansion–absorption components, such as expansion bellows, but the preferred

* Corresponding author. Tel.: +44 141 548 2046; fax: +44 141 552 5105.
E-mail address: d.mackenzie@strath.ac.uk (D. Mackenzie).

0308-0161/$ - see front matter © 2004 Elsevier Ltd. All rights reserved.
doi:10.1016/j.ijpvp.2004.09.005

Nomenclature

D	diameter of pipe cross-section	P	applied internal pressure
E	elastic modulus	p	normalised internal pressure $\mathrm{Pr_m}/t\sigma_y$
h	pipe bend factor $R_b t/r_m^2$	R_b	mean bend radius
L	length of straight pipe	r_m	mean radius of elbow cross-section
M	applied moment	t	elbow wall thickness
M_L	limit moment (instability/collapse)	z	moment multiplier
m_L	normalised limit moment $M_L/4r_m^2 t\sigma_y$	σ_y	yield stress
m	normalised moment $M/4r_m^2 t\sigma_y$	ν	Poisson's ratio

method is to specify a layout such that thermal expansion is absorbed by the bends in the piping system.

Pipe bends are more flexible than similar lengths of straight pipe, due to the complex deformation they exhibit under bending loads. When a pipe bend is subject to a bending load, the cross-section of the pipe changes shape from a circle to an oval, sometimes referred to as the von Karman effect [1]. The deformation of the cross-section may enhance or reduce the strength and stiffness of the bend, depending on the direction of the moment. When the bend is pressurised, the behaviour becomes more complex again, due to coupling between the pressure and bending responses.

When a pressurised pipe bend is subject to a bending moment, the pressure acts against the ovalisation deformation. Rodabaugh and George [2] presented the first coupled pressure–bending analysis in 1957, in which a linear work term was included in an energy analysis of a bend under an in-plane moment. However, Crandall and Dahl [3] showed that the relationship between pressure and ovalisation is non-linear, even for small deformation of the cross-section. Thus, the small displacement theory of [2] does not describe the true nature of the pressure–bending effect, although it is included as an option in some piping design codes.

1.1. Inelastic analysis of pipe bends

Much of the recent work on the behaviour of pipe bends has been based on plastic analysis and, in particular, limit load concepts. Theoretical limit analysis assumes an elastic-perfectly plastic material model and small deformation theory. The theoretical limit load is the load at which such an idealised structure can no longer maintain equilibrium with externally applied loads. Limit analysis provides a robust failure load definition provided the basic assumption of small deformation theory is appropriate.

When a structure experiences large deformations during loading, the load carrying capacity may be reduced or enhanced. When a pipe bend is subject to a closing moment its cross-section flattens, reducing the capacity of the bend to resist moment loading. This effect is called *geometric weakening*. Opening moments have the opposite effect, increasing the depth of the cross-section and increasing the resistance to bending. This behaviour is called *geometric strengthening*. These effects can be accounted for in design if large deformation (or non-linear geometry) effects are included in an inelastic analysis.

The literature on inelastic analysis of pipe bends under single and combined loads has recently been reviewed by Shalaby and Younan [4] and Chattopadhyay et al. [5]. The first plastic analysis of a pipe bend under in plane bending was a finite element method presented by Marcal [6]. Other workers, including Spence and Findlay [7] and Calladine [8], have presented analytic bending solutions based on limit theorems and plasticity theory. Goodall presented the first large deformation analysis of thin elbows under in plane bending [9] and the first lower bound solution for a thin elbow under combined loading [10]. However, Goodall's combined loading solution indicated that internal pressure reduces the limit load, which contradicted empirical observation of ductile failure. Dhalla [11] investigated modelling plastic collapse of bends by elastic–plastic shell finite element analysis, considering mesh convergence requirements, the effect of attached straight runs and the interaction between material and geometric non-linearities.

Shalaby and Younan [4] presented failure surfaces for a range of isolated 90° pipe bends subject to combined internal pressure and closing in-plane moments. The pressure and moment loads were applied simultaneously; that is, proportional loading was applied. The bends were modelled using the ABAQUS finite element program pipe bend element ELBOW31B [12], which invokes the von Karman assumption that the bending moment (and deformation) is constant along the element. This assumption neglects the effect of attached straight pipes or flanges at the ends of the bend on the deformation. The analysis assumed an ideal elastic-perfectly plastic material and large deformation theory and, consequently, different behaviour is found for closing and opening moments.

Chattopadhyay et al. [5] calculated collapse loads for a range of 90° bends with attached straight pipes under combined pressure and in-plane bending loads using the NISA 3D finite element program [13]. The piping system was modelled using 3D solid finite elements and included strain hardening and large deformation effects. The pressure

and moment loads were applied sequentially. Pressure was applied to a constant value and then the moment was applied. It is suggested that this is the most likely situation in practice, as "…pressure generally does not increase during service, whereas bending moment may increase significantly in an accidental condition." Closed-form equations for the collapse surface of the bends were formulated from the results of the finite element analysis.

The literature shows that assumptions made in the elastic–plastic analysis of pipe bends under combined loading can significantly affect the calculated ductile failure load. The object of the present paper is to investigate two related concepts in analysis of pipe bends: the basic definition of ductile failure and the effects of load history on the calculated failure load.

2. Analysis

The three piping systems considered comprise a 90° bend and two attached equal length straight pipe runs terminating at stiff flanges, as illustrated in Fig. 1. The mean cross-sectional radius of the bend and straights was set at $r_m = 250$ mm. The bend radius ratio R_b/r_m was fixed at 3 and the bend radius to thickness ratio r_m/t and bend factor ($h = R_b t/r_m^2$) were varied by changing the wall thickness, t. Three values of thickness were considered: $t = 15$, 20 and 28 mm, giving pipe bend factors, h in the range 0.18–0.336. The pipe bend geometry parameters are summarised in Table 1.

The length of the attached straight piping was chosen to ensure that the bend response was independent of the semi-rigid flanges at the end of the runs. A sensitivity analysis showed that this condition was met for all three systems for a straight length $L = 10r_m$.

An elastic-perfectly plastic material model was used in all the analyses. The material property values used were elastic modulus, $E = 200$ GN/m^2, yield stress, $\sigma_y = 300$ MN/m^2 and Poisson's ratio, $\nu = 0.3$.

2.1. Finite element modelling

The piping system configuration has two planes of symmetry and as such can be modelled by a quarter finite element mesh, with appropriate symmetry boundary conditions applied.

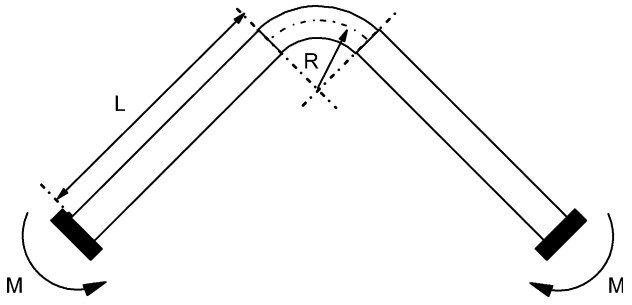

Fig. 1. Pipe bend attached to two straight runs subject to in-plane bending.

Table 1
Pipe bend geometry parameters

Mean radius, r_m (mm)	Thickness, t (mm)	r_m/t	R_b/r_m	Pipe bend factor, h
250	15	16.67	3	0.18
250	20	12.50	3	0.24
250	28	8.93	3	0.336

The systems were modelled in ANSYS [14] using plastic shell elements SHELL43. A convergence study was performed to establish a suitable mesh density for the model. The finite element mesh used in the study is shown in Fig. 2. The bend was discretised by 15 elements along the straight run, eight elements along the (half) bend and 24 elements around the half-pipe circumference. The flanges were simulated by elastic beam elements BEAM4 with elastic modulus an order of magnitude greater than the pipe material. A web of radial beam elements from the centre of the pipe-end to the flange was included to allow the bending moment to be applied as a point load at the centre of the end.

The bend is subject to in-plane moment and pressure loading. The moment was applied as a point load to the node at the centre of the web of beams at the end of the straight. The system was assumed to be closed at the ends, such that the internal pressure gives rise to an axial thrust in the system. This was applied to the flange as an edge pressure, which remains normal to the end of the pipe during deformation. Three loading sequences were considered in the investigation. In proportional loading, the internal pressure and moment are applied to the model simultaneously. In P–M loading, the internal pressure is applied to a pre-determined value then held constant as the moment is applied. In M–P loading, the moment is applied to a pre-determined value then held constant as the internal pressure is applied. Moment–pressure interaction surfaces were constructed by performing elastic–plastic analysis of each piping system for 13 different load combinations, ranging from bending only to pressure only.

2.2. Definition of failure load

Several terms are used in the literature to define the ductile or inelastic collapse load of pressurised components,

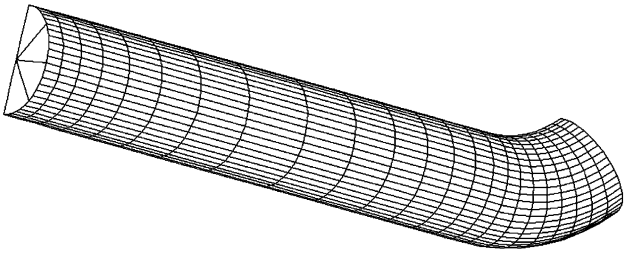

Fig. 2. Finite element mesh.

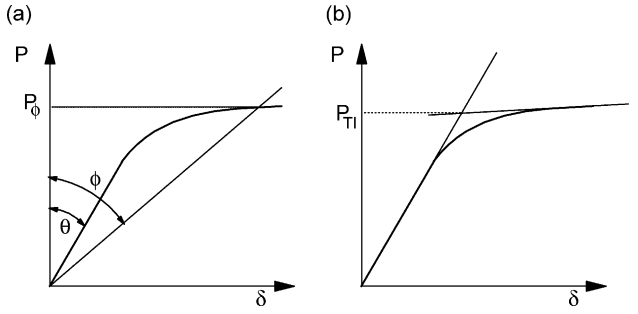

Fig. 3. (a) Twice elastic slope method, (b) tangent intersection method.

such as pipe bends and piping systems. The theoretical limit load of a structure is a well-defined concept. It is calculated by limit analysis, which assumes perfect plasticity and small deformation theory. However, in practice the expression 'limit load' is often used in a general sense to define the load at which ductile failure occurs, as observed experimentally or calculated by elastic–plastic analysis including strain hardening and/or large deformation theory. In this paper, the definitions of plastic failure mode proposed by Gerdeen [15] are used.

The *limit load* denotes the theoretical limit load in accordance with the definition of limit analysis. The limit load is the maximum load satisfying equilibrium between external and internal forces under these conditions. The theoretical limit load is independent of the load path leading to collapse.

The *plastic instability load* is a structural instability load that depends on the yield strength of the material and the influence of significant changes in shape of the structure. Calculation of this load requires large deformation effects to be included in an elastic–plastic analysis. Gerdeen states that "At the plastic instability load the load–deflection curve is characterised by zero slope (horizontal tangent)." This state may not actually be achieved in load-controlled non-linear finite element analysis, as the solution may fail to converge whist the characterising load–deformation curve has a non-zero slope. Here, the plastic instability load is taken as the last converged solution in an elastic–plastic analysis including large deformation effects. Depending on the particular structural configuration, the plastic instability load may be dependent on the load path leading to collapse.

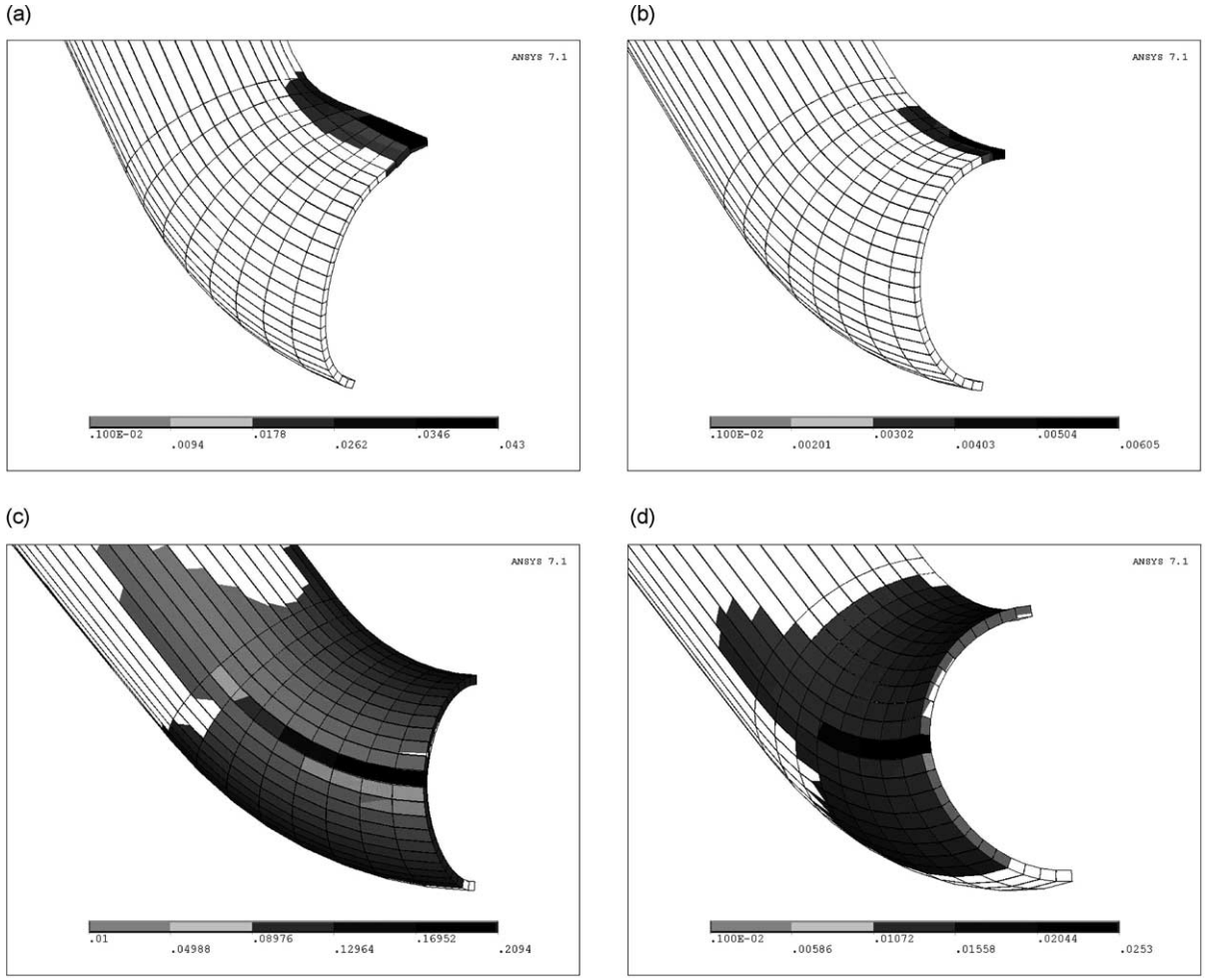

Fig. 4. von Mises equivalent plastic strain distribution at failure: (a) pressure only limit analysis, (b) pressure only large deformation analysis, (c) moment only limit analysis, (d) moment only large deformation analysis.

Gerdeen defines the *plastic load* as the load at which "…significant plastic deformation occurs…", determined by applying a *criterion of plastic collapse* to a characteristic load–deformation curve for the structure. Plastic analysis may include strain hardening effects, large strain theory and large deformation theory, at the discretion of the analyst. As in the case of plastic instability load, the plastic load depends on the order in which the loads are applied.

Several criteria of plastic collapse have been proposed for pressure vessel design. The ASME Boiler and Pressure Vessel Code Section VIII Div 2 [16] specifies use of the *Twice Elastic Slope* (TES) criterion. This is a graphical criterion in which load is plotted as the ordinate and deformation as the abscissa, as illustrated in Fig. 3a. The plastic collapse load is defined by plotting a straight line from the origin with twice the slope of the initial elastic response: that is $\tan\phi = 2\tan\theta$. The plastic load P_ϕ is that corresponding to the intersection point of the curves. Guidelines on the choice of deformation parameter are given by Gerdeen [15]. The TES criterion was used by Chattopadhyay et al. [5] to define plastic loads. Shalaby and Younan [4] used a similar criterion to define plastic loads. In their double angle method, a line is taken from the origin at twice the angle of the initial elastic response (with respect to the load axis), such that $\phi = 2\theta$. Shalaby and Younan also calculated plastic instability loads in accordance with Gerdeen's definition.

In the present investigation, it was found that the twice elastic slope criterion could not be applied to a large number of configurations, as the instability load was reached before the collapse limit line intersected the load–deformation curve. An alternative plastic collapse criterion was therefore used to define plastic load: the tangent intersection method [15]. The tangent intersection method defines the plastic collapse load as the point of intersection of tangents drawn to the initial elastic and final plastic responses of the structural response curve, as illustrated in Fig. 3b.

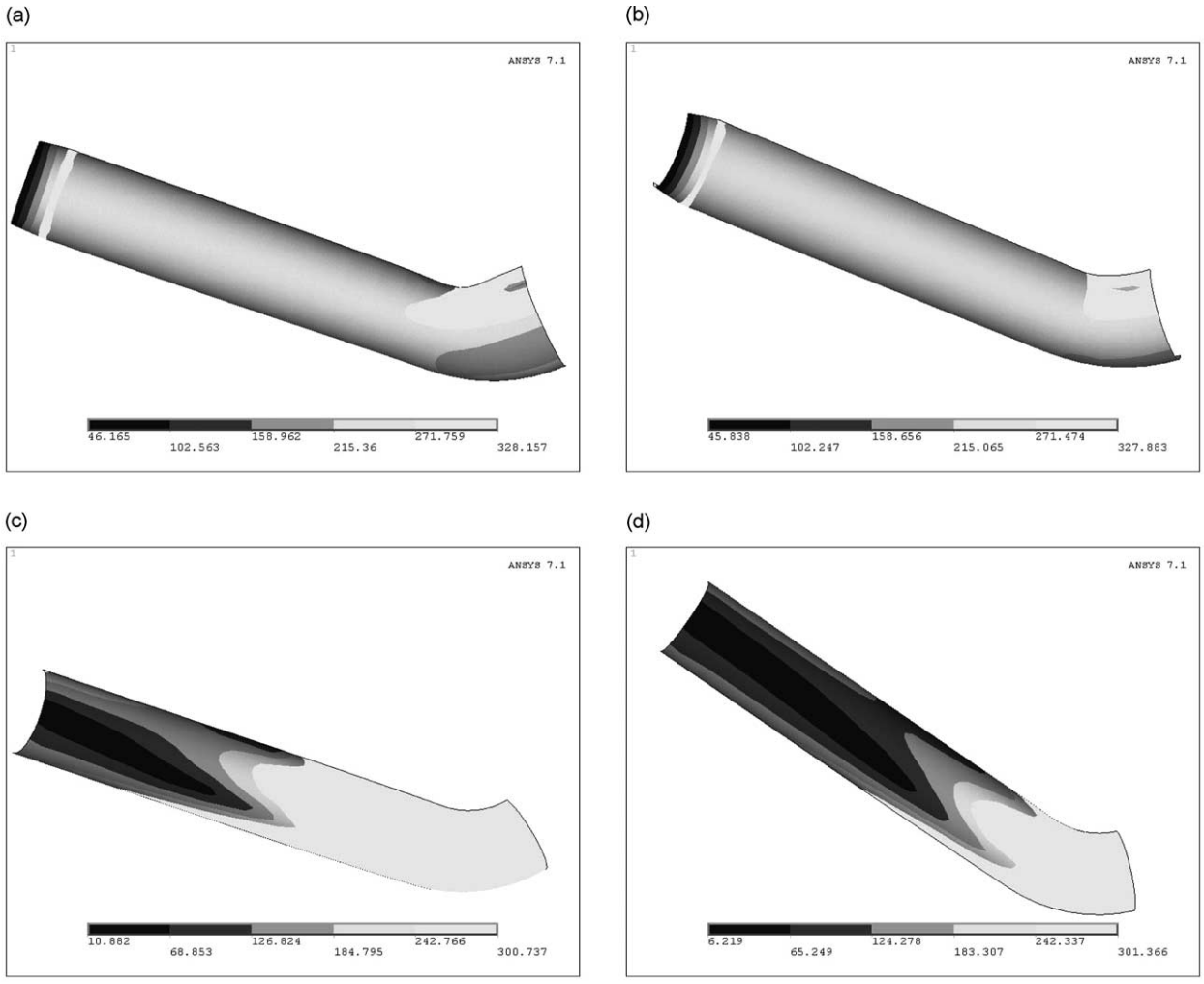

Fig. 5. von Mises equivalent stress distribution at failure: (a) pressure only limit analysis, (b) pressure only large deformation analysis, (c) moment only limit analysis, (d) moment only large deformation analysis.

3. Results

The results of the analyses are presented in non-dimensional form. Internal pressure, P, is normalised with respect to the hoop stress of a thin walled cylinder, such that the normalised pressure p is

$$p = \frac{Pr_m}{\sigma_y t}$$

Moment, M, is normalised with respect to the limit moment of a straight pipe under pure bending, such that normalised moment m is

$$m = \frac{M}{4r_m^2 \sigma_y t}$$

3.1. Pressure-only and bending-only loading

The piping systems fail by different collapse mechanisms under pressure-only and bending-only loads. The equivalent plastic strain distributions in the bend region at collapse for the small and large deformation solutions are shown for the $h=0.24$ system in Fig. 4. Under pressure-only loading, first yield occurs in the middle of the bend at the intrados. As pressure increases, the plastic zone spreads along the bend towards the junction with the straight run. There is also some limited plastic redistribution in the circumferential direction but at failure, unstable or gross plastic deformation is restricted to a relatively small plastic zone around the intrados, as shown in Fig. 4a and b for small and large deformation analyses, respectively. The calculated limit pressure (small deformation collapse load) was close to that of a straight pipe. The plastic instability pressure (large deformation collapse load) was very close to the limit pressure (about 2% lower). This indicates that large deformation effects are not significant in pressure-only loading.

The evolution of the plastic failure mechanism under bending-only loading is distinctly different from the pressure-only case. First yield occurs in the middle of the bend at the crown and, as the load is increased, the plastic zone spreads both axially along the crown towards the straight run and circumferencially outwards, towards the extrados and the intrados. Almost the entire bend experiences plastic deformation before failure occurs, as shown in Fig. 4c and d for small and large deformation analyses, respectively. The limit moment of the bend was significantly lower than the limit moment of a similar straight pipe. Further, the limit and plastic instability loads differ significantly. In the $h=0.24$ bend, plastic instability collapse occurred at around 80% of the limit load, indicating that large deformation effects significantly influence the response.

Contour plots of the von Mises equivalent stress at the outer surface of the $h=0.24$ system are shown in Fig. 5 for pressure and moment only loading, large and small deformation theory. (The maximum stress shown on the plots appears to exceed σ_y due to the stress-plotting algorithm: perfect plasticity was assumed throughout.) These figures clearly illustrate the different forms of ductile failure mechanism that occur under pressure and moment only loading.

3.2. Combined loading limit loads

In limit theory, the limit load is path independent; that is, independent of the loading sequence. This was verified for the finite element model used in the investigation by calculating the limit load of the $h=0.24$ bend for the three load sequences. Limit load surfaces obtained for proportional loading, P–M loading and M–P loading are shown in Fig. 6a. The curves are almost coincident for most of the pressure range but there is a difference between the P–M curve and the others at high values of pressure/low values of moment. In the normalised moment range 0–0.25, the pressure on the proportional loading and M–P limit surfaces exceed the limit pressure of the vessel. In the case of P–M loading, the maximum initial pressure that can be applied is, by definition, the limit pressure. Consequently, the behaviour shown by the other loading sequences cannot be obtained for P–M loading. The slight differences around the limit pressure region are due to numerical effects in the non-linear solution.

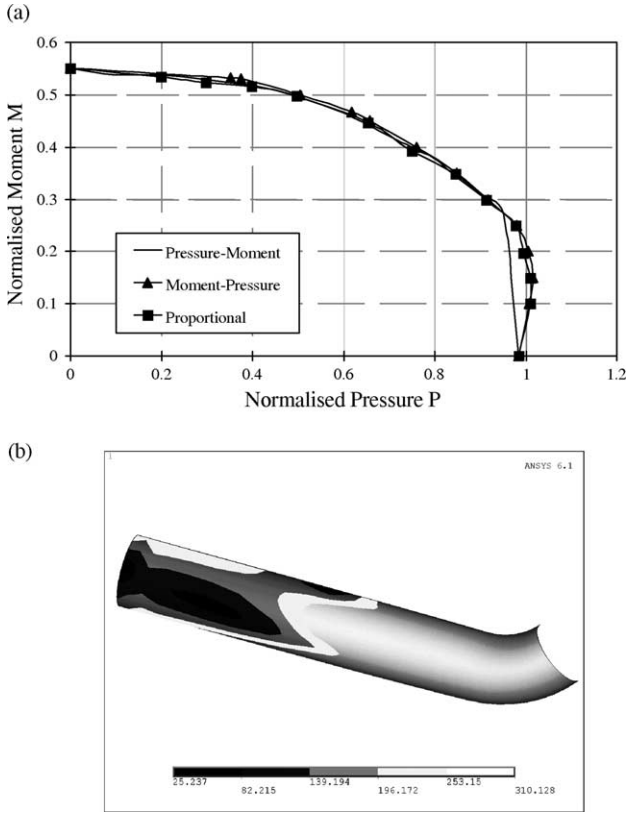

Fig. 6. (a) Limit load surfaces for the $h=0.24$ bend evaluated by proportional and sequential loading. (b) Von Mises stress distribution at limit load, $P=10$ MPa and $M=756$ kN m.

A contour plot of the von Mises equivalent stress at limit collapse ($P=10$ MPa and $M=756$ kN m) is shown in Fig. 6b. The stress distribution at collapse is similar to the moment loading limit analysis stress distribution shown in Fig. 5c.

3.3. Combined loading instability loads

In plastic instability analysis, the failure load is path dependent. Plastic instability load surfaces are shown in Fig. 7a–c for the $h=0.18$, 0.24 and 0.36 systems, respectively. Proportional loading, P–M loading and M–P loading curves are compared with the limit load surface.

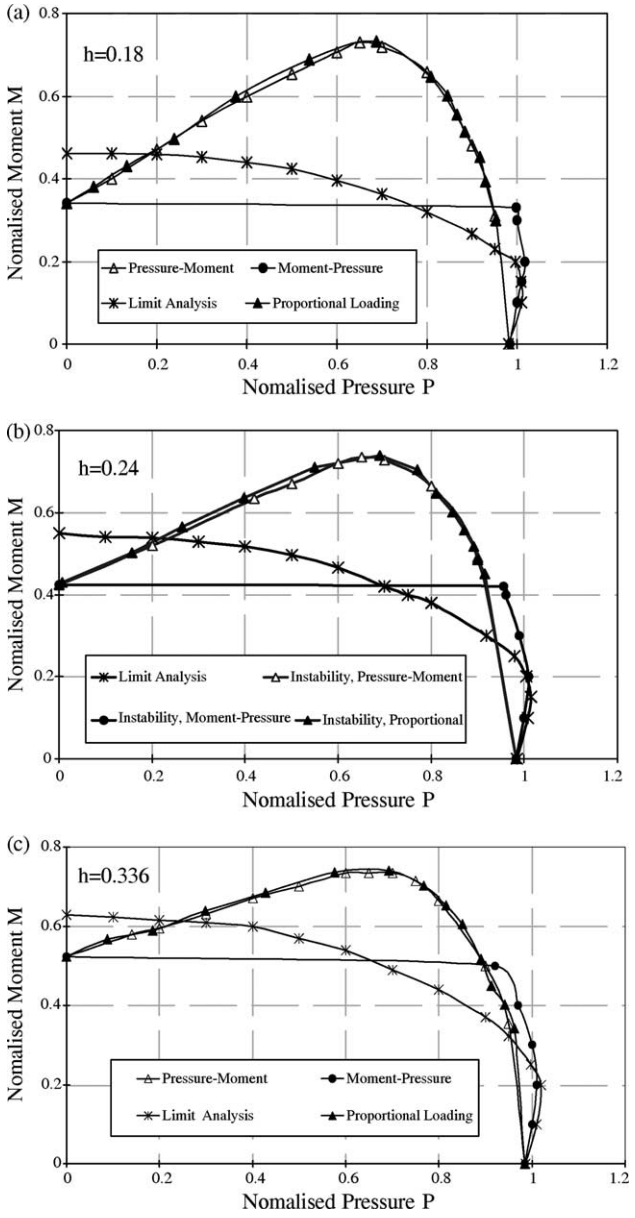

Fig. 7. Plastic instability load surfaces for the (a) $h=0.18$, (b) $h=0.24$, (c) $h=0.36$ (limit load surface shown for comparison).

Clearly, the order of loading significantly affects the calculated collapse load.

The proportional loading and P–M loading sequences give very similar failure surfaces. At low normalised pressures (less than 0.2), the ovalisation of the cross-section leads to instability at loads below the limit load; that is, the structure exhibits geometric weakening. As the pressure increases, the ovalisation is countered by the internal pressure, which seeks to expand the cross-section as a uniform circle. At normalised pressures above 0.2, significant geometric strengthening is observed but reduces as the limit pressure is approached.

The M–P loading sequence gives a distinctly different failure surface to the proportional and P–M load sequences. Under the M–P load sequence, the initial bending moment causes the section to ovalise. Subsequent pressurisation counters the ovalisation until the cross-section becomes essentially circular and, as pressure increases, a failure mechanism similar to the pressure-only mechanism forms. The form of this mechanism is effectively independent of the initial bending load.

3.4. Combined loading plastic loads

Plastic loads are defined by applying a specific criterion of plastic collapse to a characteristic load–deformation curve obtained by plastic analysis (incorporating strain hardening and/or large deformation effects). Following guidance from Gerdeen [15], the characteristic response curves for proportional and P–M loading were moment/end–rotation curves. For proportional loading, the moment was plotted against rotation of the flange for the full range of moment load applied. For P–M sequential loading, the pressure was initially applied to a constant value. This caused minor rotation of the flange. The moment was

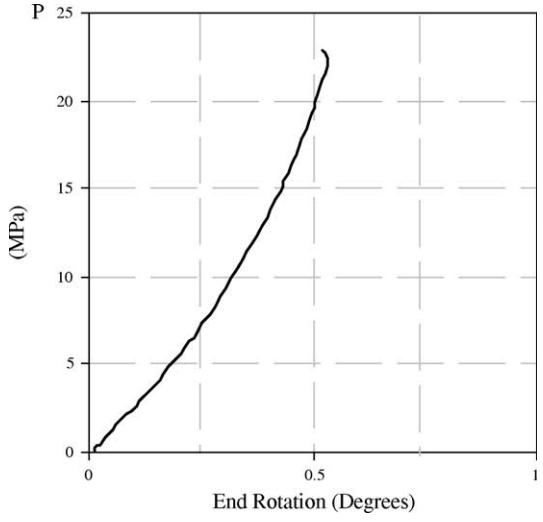

Fig. 8. Typical pressure–rotation curve from moment–pressure large deformation analysis.

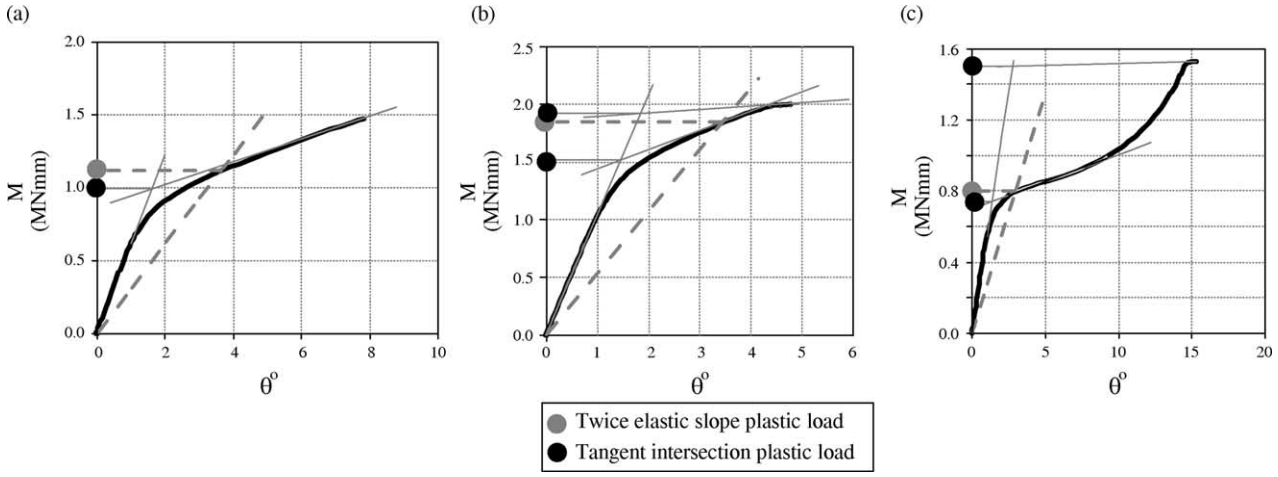

Fig. 9. Typical load–deformation curves showing twice elastic slope and possible tangent intersection constructions.

then applied and a moment–rotation curve plotted, taking the initial pressure induced rotation as a datum.

In the M–P load sequence, an initial constant moment is applied and then the pressure is increased until collapse occurs. The most significant load parameter in this case is probably pressure (the methodology is subjective) and, following Gerdeen's recommendations, the appropriate deformation parameter is change in volume. Unfortunately, change in volume is not calculated in a conventional structural analysis and an alternative deformation is required. It was decided to use end rotation as the deformation parameter for M–P loading. The initial moment was applied to a constant value. The pressure was then applied and a moment–rotation curve plotted, taking the initial moment induced rotation as a datum. A typical pressure–rotation curve is shown in Fig. 8. The curve does not include the initial rotation due to application of the moment. In practice, the initial rotation may be significantly greater than the subsequent changes in rotation when the pressure is applied. Clearly, it is not possible to apply either the twice elastic slope or tangent intersection constructions to such a plot. For this reason, no plastic loads were calculated for M–P loading.

The characteristic load–deformation curves obtained for proportional and P–M loading for the configurations considered had a wide range of forms. Fig. 9a–c shows three typical response curves. Fig. 9a shows a smooth curve with a gradual transition from elastic behaviour to steady-state plastic behaviour. The plastic pressures obtained by applying the twice elastic slope and tangent intersection methods are unambiguously defined for this response and indicated on the figure. Fig. 9b shows a different form of curve, in which the plastic response has two distinct regions with different slope. In this case, the tangent could be drawn from either slope, so there is some doubt as to which is the appropriate plastic pressure. Fig. 9c poses a different problem. The plastic response is initially concave for most of the curve but exhibits a short horizontal plateau just before failure. Large differences in plastic pressure may be obtained in this case, depending on how the criterion is applied.

It was found that for a large number of load combinations, the twice elastic slope criterion could not be applied as instability collapse occurred before the collapse limit line and load–deformation curve intersected. It was therefore decided to use the tangent intersection criterion to define plastic loads. Given the variation in form of characteristic curve encountered, it was not possible to define a consistent approach to applying the tangent intersection criterion to the whole range of configurations. Defining the tangent point and hence plastic load was therefore, to various degrees, subjective.

The plastic load surfaces obtained by applying the tangent intersection method to the proportional loading and P–M loading curves for bend $h=0.24$ are shown in Fig. 10. The two plastic load curves are similar for low pressure but clearly differ as the normalised pressure exceeds 0.8. The differences between the two plastic load curves indicate that they do not give a consistent measure of plastic load for the configurations considered.

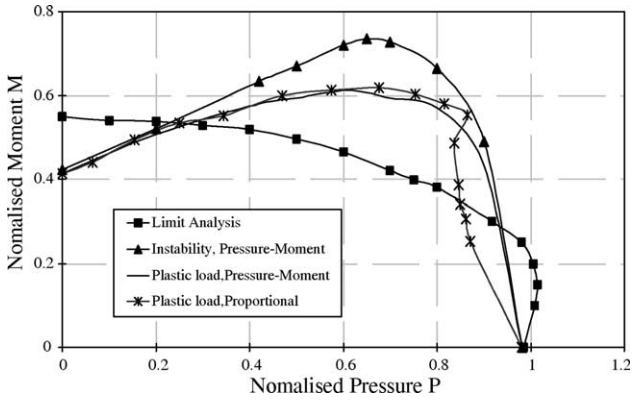

Fig. 10. Plastic loads for large deformation proportional and pressure–moment loading. Limit and plastic instability loads shown for comparison.

4. Discussion

The limit load, M–P plastic instability load, P–M plastic instability load and P–M plastic load surfaces are compared with the plastic loads given by Shalaby and Younan [4] and Chattopadhyay et al. [5] in Fig. 11. The Chattopadhyay solution for $h=0.18$, Fig. 11a, is from their closed form solution, as their FE results do not include this size of bend.

The Shalaby and Younan plastic loads are lower than the other plastic load curves as expected, as these results are for an isolated bend under pure bending, which does not benefit from the strengthening effect of attached straight pipes. The P–M plastic load curves from the present investigation and Chattopadhyay results can be compared as both are for bends with attached straights. The curves are, in fact, similar for most of the load combinations considered. At low values of pressure, the plastic load is less than the limit load. As pressure increases, geometric strengthening is observed up to almost pressure-only failure load evaluated in the present investigation. In the P–M plastic load, the failure surface in closed at a maximum plastic pressure. The Chattopadhyay plastic load decreases slightly as the pressure approaches the limit pressure but does not fall to zero, due to strain hardening (included in the analysis).

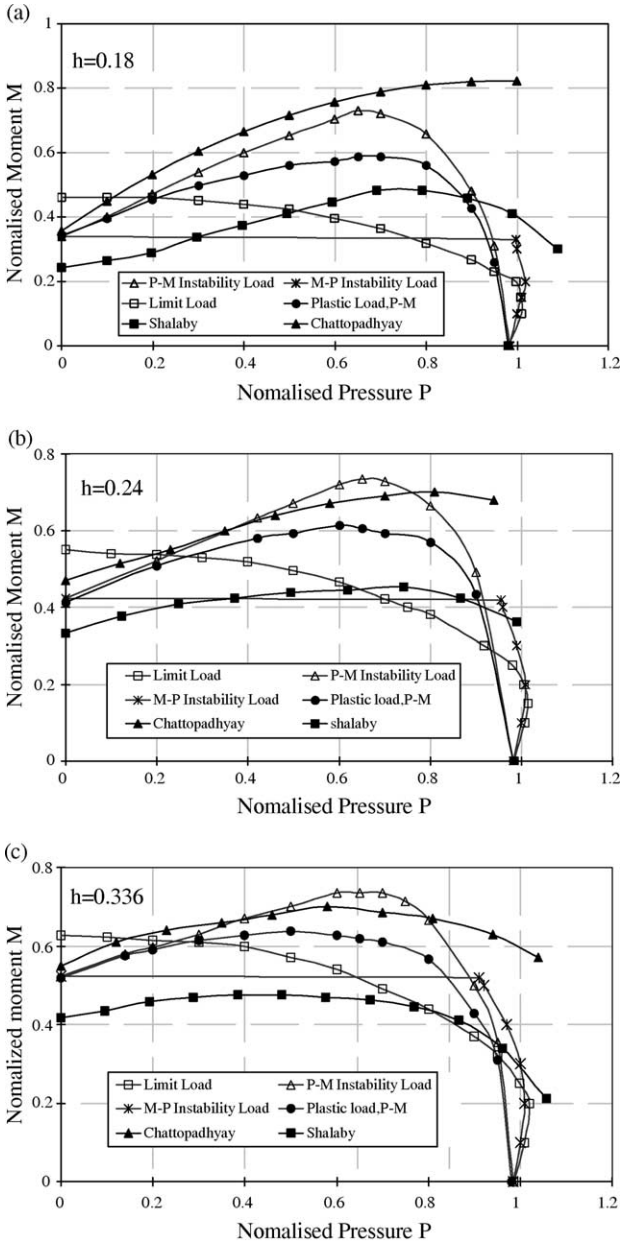

Fig. 11. Limit load, plastic instability load and plastic load surfaces compared with Shalaby and Younan [4] and Chattopadhyay et al. [5]: (a) $h=0.18$, (b) $h=0.24$, (c) $h=0.36$.

The plastic load and the P–M plastic instability load are similar for low pressures but differ greatly in the region where geometric strengthening is most pronounced, from around $p=0.1$ to 0.6. The plastic criterion effectively truncates most of the geometric strengthening effect experienced by the bend.

The M–P plastic instability load surface is distinctly different to the other curves, showing geometric weakening for the full load range. This form of loading is unlikely in practice but it may be important to note this effect in some situations.

5. Conclusions

The results of the investigation show that geometric non-linearity is a significant consideration when calculating plastic failure loads of pipe bends subject to combined loading. Significant geometric weakening is observed when the closing bending moment dominates. At higher pressures, both P–M loading and proportional loading cause considerable geometric strengthening. Calculating plastic loads for the systems proved to be problematic. Plastic loads could not be defined for M–P loading when rotation was used as a deformation parameter, due to the general form of the characteristic response curve. Many different forms of characteristic curve were obtained for P–M loading and proportional loading. The twice elastic slope criterion could not be applied to the full range of configurations and plastic load was determined by applying the tangent intersection method. It was found that significant variation in calculated plastic pressure was possible, depending on how the criterion was interpreted. The P–M and proportional load cases gave similar plastic instability failure surfaces but when the tangent intersection method was applied they gave distinctly different plastic load failure surfaces. This demonstrates that the calculated plastic load depends on the evolution of the failure mechanism rather than the actual state of collapse.

Acknowledgements

The authors thank Prof. Jim Rhodes for his help during the course of this work.

References

[1] Von Karman T. Uber die formanderung dunnwandiger rohere, insbesondere federnder ausgleichrohre. Z Vereines Dtsch Ing 1910; 55:1889–95 [in German].
[2] Rodabaugh EC, George HH. Effect of internal pressure on flexibility and stress intensification factors of curved pipes or welded elbows. J Appl Mech 1956;79:939–48.
[3] Crandall SH, Dahl NC. The influence of pressure on the bending of curved tubes. Proc Ninth Int Conf Appl Mech 1957;6:331–43.
[4] Shalaby MA, Younan MYA. Limit loads for pipe elbows under in-plane closing bending moment. ASME J Pressure Vessel Technol 1998;120:35–42.
[5] Chattopadhyay J, Nathani DK, Dutta BK, Kushwaha HS. Closed-form collapse moment equations of elbows under combined internal pressure and in-plane bending moment. ASME J Pressure Vessel Technol 2000;122:431–6.
[6] Marcal PV. Elastic–plastic behaviour of pipe bends with in-plane bending. J Strain Anal 1967;2(1):84–90.
[7] Spence J, Findlay GE. Limit load for pipe bends under in-plane bending. Proceedings of the second international conference on pressure vessel technology, San Antonio; 1973. p. 393–9.
[8] Calladine CR. Limit analysis of curved tubes. J Mech Eng Sci 1974; 16(2):85–7.
[9] Goodall IW. Large deformations in plastically deformed curved tubes subjected to in-plane bending. Research Division Report RD/B/N4312. UK: Central Electricity Generating Board; 1978.
[10] Goodall IW. Lower bound limit analysis of curved tubes loaded by combined internal pressure and in-plane bending moment. Research Division Report RD/B/N4360. UK: Central Electricity Generating Board; 1978.
[11] Dhalla AK. Plastic collapse of a piping elbow: effect of finite element convergence and residual stresses. Proc Fourth Int Conf Pressure Vessel Technol 1980;11:243–9.
[12] ABAQUS. Standard User's Manual, vol. 2.
[13] NISA. A general purpose finite element program, Windows NT/95 Production Version. ML: Engineering Mechanics Research Center; 1997.
[14] ANSYS V6.1 & V7.1, 2002 & 2003. ANSYS, Inc., Canonsberg, PA, 15317.
[15] Gerdeen JC. A critical evaluation of plastic behaviour data and a united definition of plastic loads for pressure components. WRC Bulletin 254; 1979.
[16] ASME. ASME Boiler & Pressure Vessel Code 1998. New York: The American Society of Mechanical Engineers.